

Zero Group Velocity Nonlinear Ultrasonics for Fatigue Crack Detection

Runye Lu and Yanfeng Shen*

University of Michigan-Shanghai Jiao Tong University Joint Institute, Shanghai Jiao Tong University, Shanghai, China, 200240.

ABSTRACT

This paper reports an enhanced nonlinear ultrasonics methodology leveraging zero group velocity (ZGV) mode for fatigue crack detection. The conventional nonlinear ultrasonics has been widely investigated as a promising tool for monitoring incipient damage due to its high sensitivity. Nevertheless, such methodologies face significant challenges as nonlinear signatures are vulnerable to various sources of interferences, including electronic noise, actuator bonding artifacts, and distributed material nonlinearity. To address these limitations, this paper harnesses the ZGV mode to amplify the second harmonic signal features at fatigue cracks. ZGV modes are endowed with unique characteristics of a zero-value group velocity with a finite wavenumber, triggering a localized resonance and confining the wave energy in the vicinity of a fatigue crack, which greatly enhance the signal nonlinear features. This work is structured as follows: firstly, theoretical fundamentals of ZGV Lamb modes are delineated for preparing the investigation. Then, half-ZGV frequency is selected for wave actuation, targeting at generating the second harmonic at the ZGV resonance. Finite element simulations demonstrate that half-ZGV frequency actuation triggers the ZGV resonance at the fatigue crack, thus considerably enhancing the second harmonic features compared to the standard actuation. Furthermore, the superb caliber of such a method is further demonstrated by several peculiar characteristics of the nonlinear ZGV generation from temporal, spectral, and spatial perspectives. This paper finishes with concluding remarks and suggestions for future work.

Keywords: Lamb waves; zero group velocity mode; nonlinear ultrasonics; second harmonics; nondestructive evaluation; fatigue crack

1 INTRODUCTION

Nonlinear ultrasonic methodologies, typically utilizing nonlinear features like second harmonics, mixed-frequency responses, and subharmonics, have been extensively investigated as a powerful tool for the detection of incipient damage, such as fatigue cracks, bolt loosening, delamination, etc. [1-5]. Nevertheless, these nonlinear features are inherently weak and susceptible to deceptive interferences from instrumental nonlinearity, distributed material nonlinearity, and bonding layer nonlinearity, resulting in misinterpretations and false alarms of fatigue cracks [6, 7].

To overcome these challenges, researchers have developed various strategies to enhance the efficacy of nonlinear ultrasonics. These approaches generally fall into two categories: on one hand, the elimination of undesired nonlinearity, and on the other hand, the amplification of damage nonlinearity. Shen et al. exploited metamaterials to filter away the nonlinearity from the instrument and adhesive layers [8]. Similarly, a meta-screen was designed with customized bandgap to allow the pass of fundamental waves and suppress the second harmonics generated by deceptive nonlinear sources by Cheng et al. [9]. Regarding the enhancement of damage-related nonlinearity, meta-structures were employed for converting S_0 to A_0 to magnify the second harmonic component [10, 11]. Nonlinear acoustic phenomena, such as cumulative effect [12], binding condition [13], and internal resonance criterion [14], were leveraged for the same purpose. Additionally, the advanced nonlinear indicators such as the sideband peak count index (SPC) proposed by Kundu et al. were exploited to improve the nonlinear ultrasonic performance [15].

Different from previous endeavors, this research develops a novel approach to magnify the sensing signal nonlinear features by leveraging zero group velocity (ZGV) modes. The fundamentals of ZGV waves have been widely investigated [16]. They have been reported possessing a unique characteristic of a zero-value group velocity with a finite wavenumber, engendering a localized resonance, and thus confining the wave energy in the vicinity of its generation [17]. Current applications of ZGV modes on Structural Health Monitoring (SHM) and Nondestructive Evaluation (NDE) mainly rely on the deviation of ZGV frequencies due to either local material/geometric properties changes or damage occurrences [18,

19]. Regarding the combination of nonlinear ultrasonic and ZGV modes, pioneer research has been conducted on nonlinear ZGV generation due to dispersed material nonlinearity by counter-directional wave mixing and non-collinear wave mixing [20-22]. Yet, the integration of second harmonic generation of ZGV resonances for localized fatigue crack detection has seldom been reported. From another perspective, most techniques directly utilizing ZGV modes confine the inspection in the vicinity of actuation due to the non-propagating characteristic, which considerably limited the sensing range. To address these limitations, this study aims at facilitating a short communication on a ZGV-mode enhanced second harmonic methodology for fatigue crack detection.

This paper commences with theoretical fundamentals of the ZGV modes and obtaining the ZGV frequencies in a target aluminum plate. The obtained ZGV frequencies serve as the basis for the appropriate actuation frequency selection to facilitate the second harmonic ZGV generation at a fatigue crack. Subsequently, finite element (FE) analyses are conducted to demonstrate the second harmonic generation of ZGV resonances and the enhanced performance of the nonlinear features compared with a standard and arbitrary actuation. Ultimately, several peculiar phenomena associated with ZGV resonance generation are explored and elucidated for showcasing the prowess of the half-ZGV nonlinear ultrasonic technique for crack detection.

2 FUNDAMENTALS OF LAMB WAVE ZGV MODES

This section aims at introducing the fundamentals of the ZGV modes and provides the corresponding frequencies in an aluminum plate as the example for investigation, as depicted in Figure 1(a). The identification of ZGV modes and the determination of ZGV frequencies would be accomplished through the group velocity dispersion curves. Referring to the fundamentals of wave mechanics [23], the well-established Rayleigh-Lamb equations governing symmetric and anti-symmetric modes can be formulated as follows:

$$\frac{\tan \eta_P d}{\tan \eta_S d} = -\frac{(\xi^2 - \eta_S^2)^2}{4\xi^2 \eta_P \eta_S} \quad (\text{symmetric Rayleigh-Lamb equation}) \quad (1)$$

$$\frac{\tan \eta_P d}{\tan \eta_S d} = -\frac{4\xi^2 \eta_P \eta_S}{(\xi^2 - \eta_S^2)^2} \quad (\text{antisymmetric Rayleigh-Lamb equation}) \quad (2)$$

where d denotes the half plate thickness; $\eta_P^2 = \omega^2/c_P^2 - \xi^2$, $\eta_S^2 = \omega^2/c_S^2 - \xi^2$ and ξ signifies the wavenumber. Numerical solution of Rayleigh-Lamb equation yields the eigenvalues, $\xi_0^S, \xi_1^S, \xi_2^S, \dots, \xi_0^A, \xi_1^A, \xi_2^A, \dots$, representing the wavenumbers of the symmetric and anti-symmetric lamb wave modes. The group velocity curves can be obtained by solving the above equation and evaluating the following relation $c_g = c^2 \cdot (c - fd \cdot \partial c / \partial (fd))^{-1}$ against the frequency and half thickness product, fd .

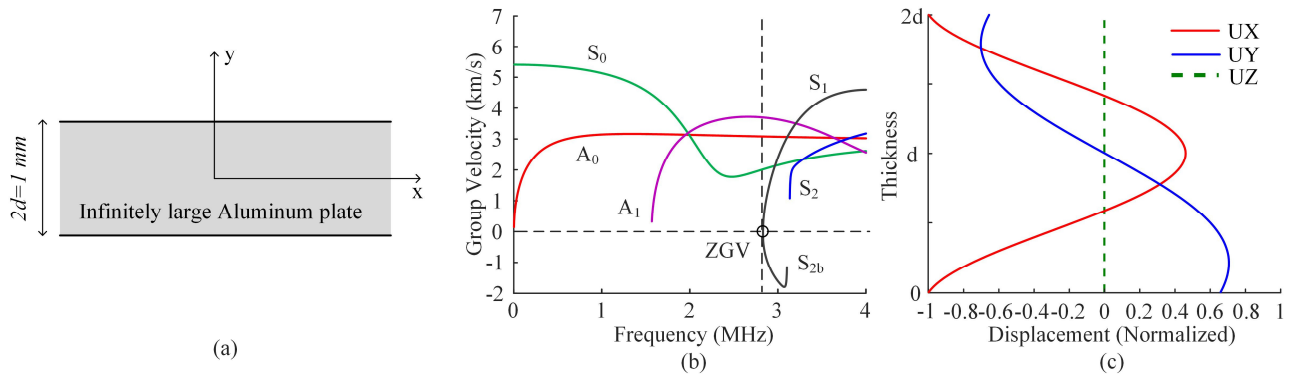


Figure 1: Fundamentals of ZGV plate modes: (a) the plate under investigation; (b) group velocity curves of the plate; (c) mode shape of the first symmetric ZGV wave.

The material properties of the aluminum plate are defined as follows: a density of 2780 kg/m³, a Young's modulus of 72.4 GPa, and a Poisson's ratio of 0.33. By numerically solving the transcendental equation, the group velocity dispersion curves are derived, as displayed in Figure 1(b). The ZGV mode can be identified by tracing the point at dispersion curves with zero group velocity value. The ZGV frequency of the target aluminum plate settles at 2726 kHz. The mode shape corresponding to the ZGV frequency is also presented in Figure 1(c). Notably, such a ZGV mode residents on the prototypical first symmetric ZGV (S₁-ZGV) resonance.

3 NUMERICAL DEMONSTRATION FOR ENHANCING NONLINEAR ULTRASONICS

An FE model was developed incorporating various damage scenarios to assess the feasibility of the ZGV-enhanced nonlinear ultrasonic methodology. The superior performance of second harmonic generation at ZGV resonance was validated by benchmarking it against excitation at an arbitrary frequency. Furthermore, several distinctive characteristics of nonlinear ZGV mode generation were examined, offering deeper insights into the underlying mechanisms that contribute to its heightened sensitivity for damage detection.

3.1 FE Model Configurations and Damage Settings

A 2D FE model of the aluminum plate, with a thickness of 1 mm, was constructed as depicted in Figure 2. The material properties of the aluminum were identical to those in the theoretical part. Absorbing layers with increasing damping (ALID) were implemented to function as the non-reflective boundary (NRB), simulating an infinitely large structure. The NRB was modeled utilizing the beta coefficient of Rayleigh damping model, following Ref. [24]. The 2-D 8 nodes rectangular element was applied. The element size a was controlled to meet the specific requirement of $a_{max} \leq \lambda_{min}/20$, where λ_{min} represents the smallest wavelength under consideration. The contact pairs, comprising of Contact 172 and Target 169, were employed to simulate the fatigue cracks, the breathing behavior of which would generate Contact Acoustic Nonlinearity (CAN). Various lengths of fatigue cracks were modeled to represent different levels of damage severity.

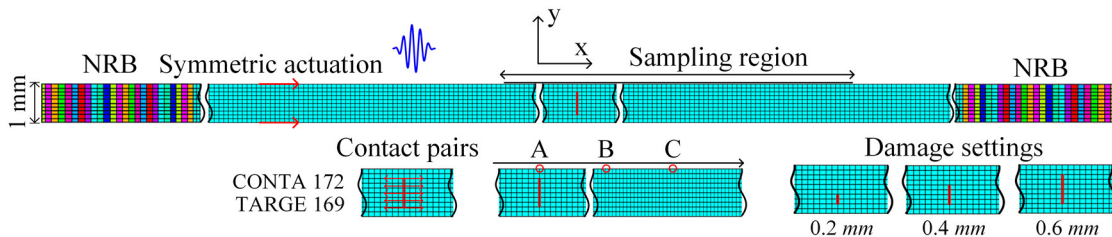


Figure 2: FE model configurations of the aluminum plate and corresponding damage settings.

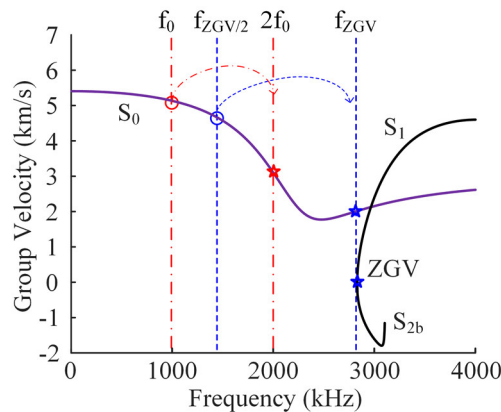


Figure 3: Selection of actuation frequencies and the corresponding second harmonic components in dispersion curves for only symmetric modes.

Regarding the actuation settings of the model, a 50-count tone burst signal was applied using the symmetric pin-force excitation. Under such configuration, only the S₀ mode would be generated. The actuation frequencies were selected as 1000 kHz (an arbitrary and standard frequency) and 1363 kHz (selective half-ZGV frequency), as illustrated in Figure 3. The half-ZGV excitation frequency could facilitate the second harmonic generation of ZGV mode at the fatigue crack. The

sampling region was positioned across the damage area to capture the temporal displacement response at sensing points along the region with a spatial interval of 0.25 mm. In terms of solution type, transient analysis was performed with a time step of 35 ns, ensuring the temporal resolution of $\Delta t \leq 1/20 f_{\max}$, where f_{\max} represents the maximum frequency component for analysis.

3.2 Verification of Localized Second Harmonic ZGV Generation at Fatigue Cracks

This subsection provides a comprehensive analysis of second harmonic ZGV generation from multiple perspectives. As the actuated guided wave packet propagates along the aluminum plate and interacts with the fatigue crack, higher harmonic signals are induced. The second harmonic at half-ZGV frequency is strategically tuned to coincide with the ZGV frequency, thereby facilitating ZGV resonance. To validate this phenomenon, the time-domain displacement responses in the y-direction at three representative locations are presented in Figure 4.

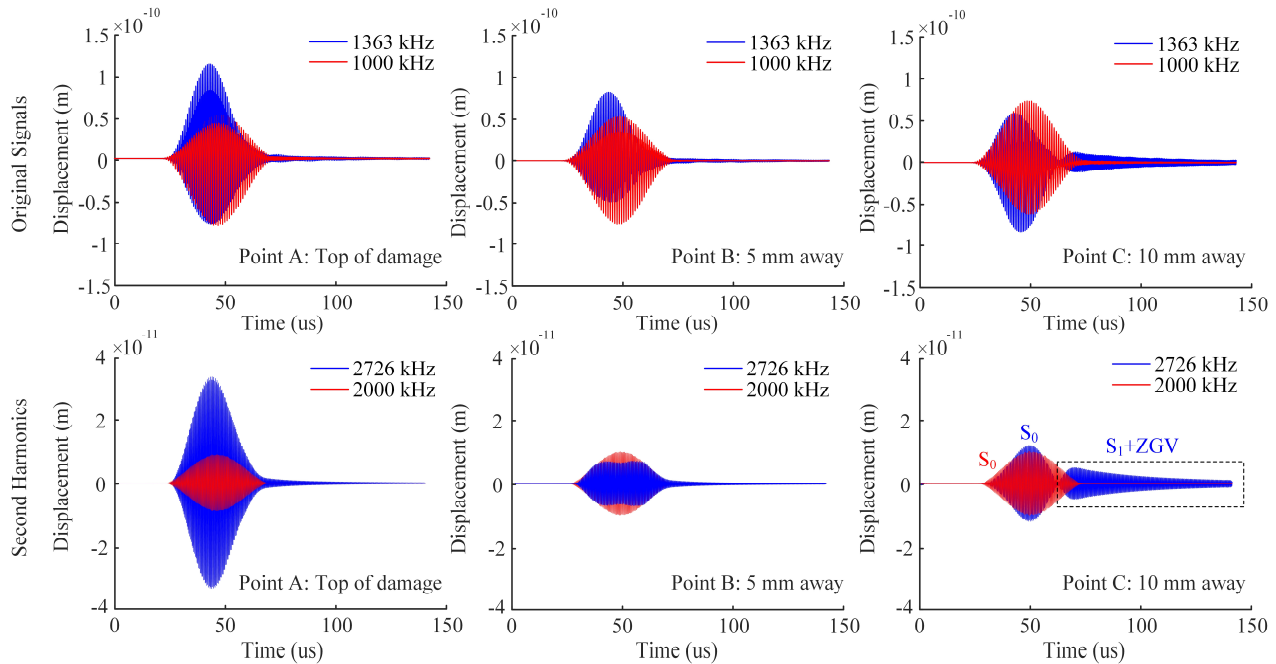


Figure 4: Temporal displacement responses of original signals (top figures) and second harmonic components (bottom figures) at point A, B, and C.

To clearly visualize the generation of ZGV modes, a band-pass filter was applied to the original signals to highlight the second harmonic component. At Point A, the half-ZGV actuation response exhibited a substantially higher amplitude than the 1000 kHz excitation, which primarily comprised S_0 and S_1 modes, as identified in the dispersion curves in Figure 3. As the wave propagated to Points B and C, the second harmonic component of the half-ZGV actuation experienced dispersion due to variations in group velocity. Notably, the S_1 -ZGV mode became increasingly dominant, manifesting as a localized resonance along the plate's thickness. This sustained resonance remained concentrated near the damage site for an extended period, giving rise to the characteristic "ringing effect." The persistence of this effect is further corroborated by the vibrational patterns observed after the fundamental wave packet dissipates, as depicted in Figure 5.

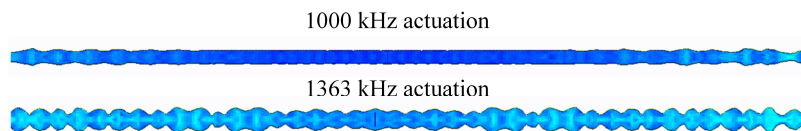


Figure 5: Vibrational pattern after fundamental wave package illustrating ringing effect.

To further confirm the presence of the S_1 -ZGV mode, temporal displacement responses within the sampling region were analyzed to derive wavenumber-frequency dispersion curves, as shown in Figure 6. For 1000 kHz excitation, only

conventional higher harmonic components at 2000 kHz and 3000 kHz were observed, lacking any distinctive features. In contrast, half-ZGV frequency actuation led to the clear emergence of second harmonic ZGV modes, distinctly highlighted within the red frame. These modes exhibited a significantly enhanced response amplitude, further substantiating the efficacy of the proposed methodology.

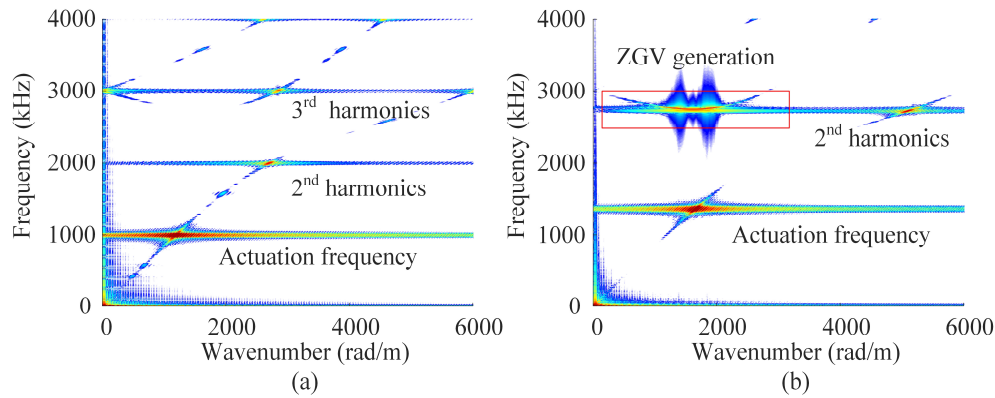


Figure 6: Wavenumber-frequency dispersion curves for (a) 1000 kHz actuation case; (b) half-ZGV frequency actuation case.

3.3 Demonstration of Enhanced Performance for Fatigue Crack Detection

Building upon the verification of ZGV mode generation, this section emphasizes the effectiveness of ZGV resonance in amplifying second harmonic signatures for fatigue crack detection. The displacement response spectra in the x- and y-directions, measured at the point directly above the fatigue crack (Point A), are depicted in Figure 7. Notably, the amplitude of the ZGV enhanced second harmonics significantly exceeded the intensity of the standard second harmonic component. The displacement amplitude at f_{ZGV} in y direction was even larger than that of fundamental frequency $f_{ZGV/2}$, due to the obvious out-of-plane component for the ZGV mode shape as shown in Figure 1. Furthermore, the nonlinear generation of ZGV modes facilitated the localized accumulation of second harmonic energy near the fatigue crack. Consequently, employing a Doppler vibrometer to measure out-of-plane displacements enables the detection of a highly amplified second harmonic response, offering exceptional sensitivity to fatigue crack presence.

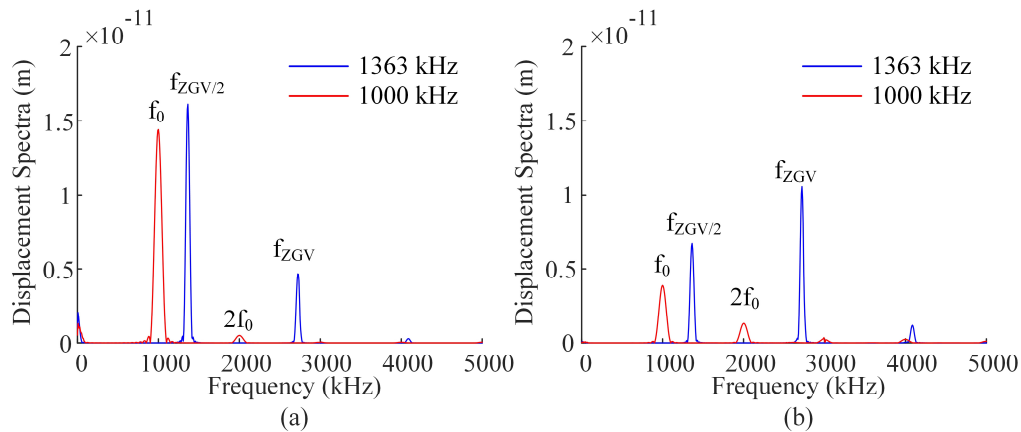


Figure 7: Comparative displacement frequency spectra for both actuations at the damage site (a) displacement in x direction; (b) displacement in y direction.

To quantify the second harmonics, a nonlinear intensity index was defined as the ratio of the second harmonic amplitude to that of the fundamental wave, represented by the following equation $\chi = A_{2f} / A_f$. The nonlinear intensity values for both actuation cases, listed in Table 1, further corroborate the enhanced performance of ZGV resonance. Notably, the second harmonic amplitude surpasses that of the fundamental frequency, resulting in an intensity factor greater than 1.

This phenomenon is seldom observed with conventional wave mode selections, highlighting the distinctive efficacy of the ZGV-enhanced methodology.

Table 1: Relative nonlinear intensity index value

Frequency	X direction	Y direction
χ : 1000 kHz	0.035	0.338
χ : 1363 kHz	0.288	1.579
Increasing Rate	722.86%	367.16%

To visualize the time-frequency responses for various damage settings, Short Time Fourier Transform (STFT) was applied to temporal displacement signals, as shown in Figure 8. The results indicate that larger fatigue cracks would induce more pronounced second harmonic generation, which can be verified by the nonlinear intensity coefficient.

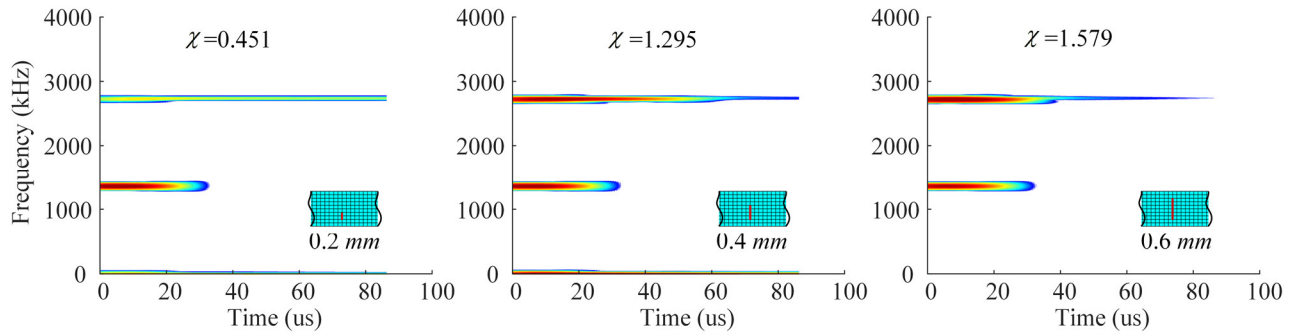


Figure 8: STFT results for three damage settings.

3.4 Informative Characteristics of Nonlinear ZGV Resonance Generation

This part investigated the distinctive features of the second harmonic generation of ZGV resonance at the crack site. The second harmonic wave energy can be estimated by the following equation, defined by the integral of displacement spectral amplitude $P(f)$ over the surrounding frequency range:

$$E = \int_{f_{2nd}} P(f) df . \quad (3)$$

As displayed in Figure 9(a), the spatial energy distribution of the second harmonic component across the fatigue crack is displayed. Generally, the spectral energy of half-ZGV actuation case (blue line) overwhelmed that of the 1000 kHz actuation case (red line), peaking at the crack site and rapidly fading away with the distance increasing. Additionally, fluctuations in spectral energy were observed along the sampling points, with the spatial interval between fluctuations corresponding to 2 mm, which is consistent with half the wavelength of the ZGV mode, as shown in Figure 9(b). These observations suggest that the ZGV generation effectively localizes wave energy in the vicinity of the crack, thereby acting as a source for second harmonic waves and significantly enhancing the amplitude of the second harmonic response.

Further, the time-space representation of the second harmonic displacement for the 1363 kHz actuation case was displayed in Figure 10. The slope of time-space plot, dt/dx , denoted the reciprocal of the wave group velocity, $1/c_g$. There existed both the propagating wave modes (with finite slope) and non-propagating ZGV mode (with infinite slope), as highlighted on the right side of Figure 10. Notably, a significantly larger displacement, resulting from ZGV resonance, is observed near the crack site throughout the entire inspection duration, indicative of the ringing effect and a zero group velocity. The spatial interval corresponding to the maximum displacement was found to be 2 mm, consistent with the previous observation in the energy distribution.

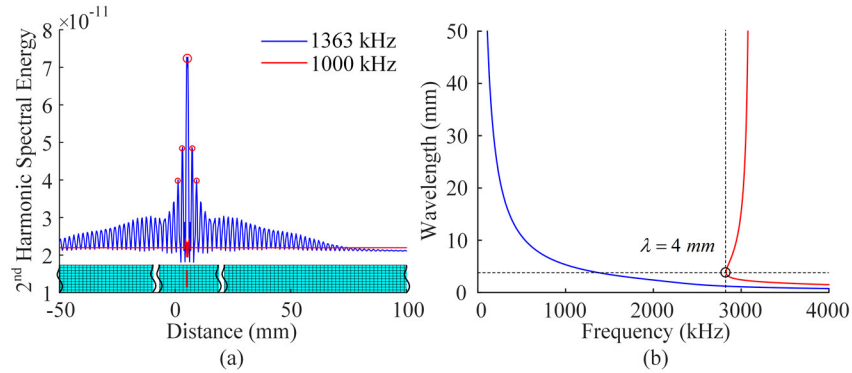


Figure 9: (a) Spectral energy distribution over the spatial sampling region; (b) wavelength curve showing a 4 mm wavelength for the ZGV mode.

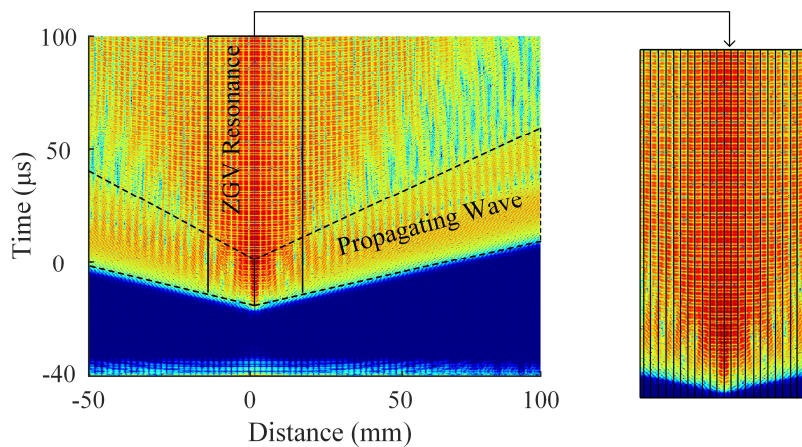


Figure 10: Time-space signal feature of second harmonic displacement for half-ZGV actuation.

It should be noted that the aforementioned distinctive nonlinear signatures can help address the challenges and influences from system inherent nonlinearities and distributed material nonlinearities. The inherent nonlinearity at the actuation site will directly be stopped by generating the second harmonic at ZGV and stay near the actuator without further propagating into the target domain of investigation. Furthermore, the localized effect would distinguish itself for fatigue crack detection, rather than a distributed nonlinear feature without accumulation.

4 CONCLUDING REMARKS AND FUTURE WORK

This paper reported a ZGV mode enhanced nonlinear ultrasonic methodology for detecting fatigue cracks. The theoretical analysis determined the ZGV mode frequency of the target plate, providing a reference for selecting optimal actuation frequencies. FE simulations demonstrated the second harmonic generation of ZGV resonances and highlighted the superior performance of half-ZGV actuation compared to arbitrary frequency excitation. Furthermore, several unique characteristics, such as energy concentration, ringing effect, and local resonance associated with second harmonic ZGV generation, were investigated from both energy and time-space perspectives. These distinctive nonlinear signatures offered a robust means to mitigate challenges arising from system-inherent and material nonlinearities.

Future work will involve an in-depth experimental investigation of the trembling features and their potential applications in structural sensing and structural health monitoring across diverse scenarios. Beyond experimental validation, the proposed method should be extended to a broader range of materials, such as carbon fiber-reinforced polymers, silicon, and glass fiber composites, as well as complex structures, including pipelines, bolted joints, and stiffened shells. Furthermore, a Doppler Laser Vibrometer will be employed to implement nonlinear ZGV ultrasonic methodologies, enabling non-contact damage detection and high-resolution imaging.

ACKNOWLEDGMENTS

The support from the National Natural Science Foundation of China (contract number 52475161) is thankfully acknowledged. Dr. Yanfeng Shen appreciates the funding from John Wu & Jane Sun Endowed Professorship.

REFERENCES

- [1] M. Zhang, Y. Shen, L. Xiao, and W. Qu, "Application of subharmonic resonance for the detection of bolted joint looseness," *Nonlinear Dynamics*, vol. 88, no. 3, pp. 1643-1653, 2017, doi: 10.1007/s11071-017-3336-1.
- [2] R. Lu, Y. Shen, B. Zhang, and W. Xu, "Nonlinear Electro-Mechanical Impedance Spectroscopy for fatigue crack monitoring," *Mechanical Systems and Signal Processing*, vol. 184, p. 109749, 2023/02/01/ 2023, doi: doi.org/10.1016/j.ymssp.2022.109749.
- [3] Z. Su, C. Zhou, M. Hong, L. Cheng, Q. Wang, and X. Qing, "Acousto-ultrasonics-based fatigue damage characterization: Linear versus nonlinear signal features," *Mechanical Systems and Signal Processing*, vol. 45, no. 1, pp. 225-239, 2014/03/03/ 2014, doi: doi.org/10.1016/j.ymssp.2013.10.017.
- [4] P. Liu, L. Yang, K. Yi, T. Kundu, and H. Sohn, "Application of nonlinear ultrasonic analysis for in situ monitoring of metal additive manufacturing," *Structural Health Monitoring*, p. 14759217221113447, 2022, doi: 10.1177/14759217221113447.
- [5] R. Lu and Y. Shen, "Entire loosening stage monitoring of bolted joints via nonlinear electro-mechanical impedance spectroscopy," *Structural Health Monitoring*, p. 14759217241289872, 2024, doi: 10.1177/14759217241289872.
- [6] S. Shan, L. Cheng, and P. Li, "Adhesive nonlinearity in Lamb-wave-based structural health monitoring systems," *Smart Materials and Structures*, vol. 26, no. 2, 2017, doi: 10.1088/1361-665x/26/2/025019.
- [7] M. H. Hafezi, R. Alebrahim, and T. Kundu, "Peri-ultrasound for modeling linear and nonlinear ultrasonic response," *Ultrasonics*, vol. 80, pp. 47-57, 2017/09/01/ 2017, doi: doi.org/10.1016/j.ultras.2017.04.015.
- [8] Y. Tian, Y. Shen, D. Rao, and W. Xu, "Metamaterial improved nonlinear ultrasonics for fatigue damage detection," *Smart Materials and Structures*, vol. 28, no. 7, 2019, doi: 10.1088/1361-665X/ab2566.
- [9] S. Shan, Z. Liu, C. Zhang, L. Cheng, and Y. Pan, "A metamaterial-assisted coda wave interferometry method with nonlinear guided waves for local incipient damage monitoring in complex structures," *Smart Materials and Structures*, vol. 33, no. 3, 2024, doi: 10.1088/1361-665X/ad254c.
- [10] Z. Liu, S. Shan, and L. Cheng, "Meta-structure enhanced second harmonic S(0) waves for material microstructural changes monitoring," *Ultrasonics*, vol. 139, p. 107295, Apr 2024, doi: 10.1016/j.ultras.2024.107295.
- [11] H. Zhou, J. Zhao, Y. Tian, I. Kovacic, and R. Zhu, "Locally resonant metamaterial for the regulation of damage-related nonlinearity based on second harmonic generation," *Nonlinear Dynamics*, vol. 112, no. 19, pp. 16771-16786, 2024/10/01 2024, doi: 10.1007/s11071-024-09933-w.
- [12] S. Shan, Y. Zhang, L. Cheng, Y. Song, Y. Pan, and L. Cheng, "'Cumulative effect' of second harmonic Lamb waves in a lossy plate," *Ultrasonics*, vol. 138, p. 107229, Mar 2024, doi: 10.1016/j.ultras.2023.107229.
- [13] H. Jin Lim, H. Sohn, and P. Liu, "Binding conditions for nonlinear ultrasonic generation unifying wave propagation and vibration," *Applied Physics Letters*, vol. 104, no. 21, 2014, doi: 10.1063/1.4879836.
- [14] J. C. Pineda Allen and C. T. Ng, "Mixing of Non-Collinear Lamb Wave Pulses in Plates with Material Nonlinearity," *Sensors (Basel)*, vol. 23, no. 2, Jan 8 2023, doi: 10.3390/s23020716.
- [15] G. Zhang, P. A. Deymier, K. Runge, and T. Kundu, "Monitoring damage growth and topographical changes in plate structures using sideband peak count-index and topological acoustic sensing techniques," *Ultrasonics*, vol. 141, p. 107354, Jul 2024, doi: 10.1016/j.ultras.2024.107354.
- [16] C. Prada, D. Clorennec, and D. Royer, "Local vibration of an elastic plate and zero-group velocity Lamb modes," *J Acoust Soc Am*, vol. 124, no. 1, pp. 203-12, Jul 2008, doi: 10.1121/1.2918543.
- [17] Y. Wu, R. Cui, K. Zhang, X. Zhu, and J. S. Popovics, "On the existence of zero-group velocity modes in free rails: Modeling and experiments," *NDT & E International*, vol. 132, 2022, doi: 10.1016/j.ndteint.2022.102727.
- [18] J. Spyttek, A. Ziaja-Sujdak, K. Dziedzic, L. Pieczonka, I. Pelivanov, and L. Ambrozinski, "Evaluation of disbonds at various interfaces of adhesively bonded aluminum plates using all-optical excitation and detection of zero-group velocity Lamb waves," *NDT & E International*, vol. 112, 2020, doi: 10.1016/j.ndteint.2020.102249.

- [19] M. Ren, X. Meng, and M. Deng, "Evaluating impact damage on carbon fiber-reinforced polymer plates utilizing zero-group-velocity Lamb waves," *Smart Materials and Structures*, vol. 33, no. 9, 2024, doi: 10.1088/1361-665X/ad6797.
- [20] P. Mora, M. Chekroun, S. Raetz, and V. Tournat, "Nonlinear generation of a zero group velocity mode in an elastic plate by non-collinear mixing," *Ultrasonics*, vol. 119, p. 106589, Feb 2022, doi: 10.1016/j.ultras.2021.106589.
- [21] W. Li, C. Zhang, and M. Deng, "Modeling and simulation of zero-group velocity combined harmonic generated by guided waves mixing," *Ultrasonics*, vol. 132, p. 106996, Jul 2023, doi: 10.1016/j.ultras.2023.106996.
- [22] C. Zhang, W. Li, and M. Deng, "Experimental observation of zero-group velocity combined harmonic generated by counter-directional Lamb wave mixing," *Ultrasonics*, vol. 143, 2024, doi: 10.1016/j.ultras.2024.107413.
- [23] V. Giurgiutiu, "Chapter 6 - Guided Waves," in *Structural Health Monitoring with Piezoelectric Wafer Active Sensors (Second Edition)*, V. Giurgiutiu Ed. Oxford: Academic Press, 2014, pp. 293-355.
- [24] P. Rajagopal, M. Drozd, E. A. Skelton, M. J. S. Lowe, and R. V. Craster, "On the use of absorbing layers to simulate the propagation of elastic waves in unbounded isotropic media using commercially available Finite Element packages," *NDT & E International*, vol. 51, pp. 30-40, 2012, doi: 10.1016/j.ndteint.2012.04.001.